

# Reversible Insertion of Unactivated Alkenes into Silicon(II)–Tin Bonds\*\*

Ricardo Rodriguez, Yohan Contie, David Gau, Nathalie Saffon-Merceron, Karinne Miqueu, Jean-Marc Sotiropoulos, Antoine Baceiredo,\* and Tsuyoshi Kato\*

The migratory insertion of alkenes is one of the most fundamental processes in organometallic chemistry and thus plays a crucial role in many catalytic processes, such as polymerization,<sup>[1]</sup> 1,2-addition reactions,<sup>[2,3]</sup> and Heck-type reactions.<sup>[4]</sup> In many cases, the insertion reaction is reversible, and a key step in catalysis is the formation of alkenes through a  $\beta$ -hydride elimination from alkyl transition-metal complexes.

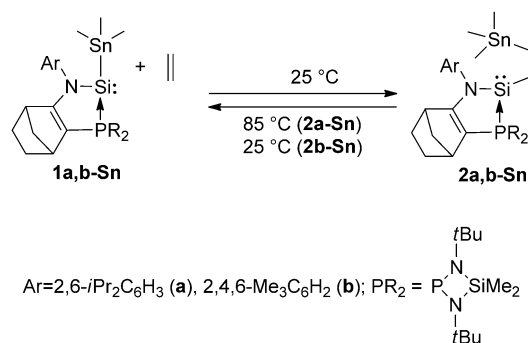
In the case of nonmetallic systems, the olefin-insertion reaction is long-known in the chemistry of Group 13 elements, as in the case of alkene hydroboration.<sup>[5,6]</sup> Olefin polymerization promoted by aluminum-based catalysts is believed to proceed through olefin insertion into an Al–C bond,<sup>[7]</sup> although the mechanism and active catalytic species are still controversial.<sup>[8]</sup> The thermal decomposition of trisopropylaluminum through  $\beta$  elimination is a well-known synthetic method involving diisobutylaluminum hydride (DIBAL).<sup>[9]</sup> In marked contrast, similar chemistry of Group 14 elements is underdeveloped. Only a few hydrostannylation<sup>[10]</sup> and hydrogermylation<sup>[11]</sup> reactions of unsaturated compounds with tin(II) or germanium(II) hydrides<sup>[12]</sup> have recently been reported. It was also reported that the hydrogermylation reaction of a phosphalkyne is reversible.<sup>[13]</sup>

We recently developed stable silylene–phosphine complexes, which showed high reactivity as silylenes<sup>[14]</sup> and as phosphonium silaylides.<sup>[15]</sup> In particular, we reported that they react reversibly with unactivated alkenes, such as ethylene, in a [2+1] cycloaddition process.<sup>[16]</sup> Furthermore, in the case of the silicon(II) hydride derivative **1a-H** (named in analogy with **1a-Sn** in Scheme 1), the oxidative addition was followed by a migratory insertion of the alkene into the Si–H bond to

regenerate a reactive Si<sup>II</sup> species.<sup>[17]</sup> This reaction can be regarded as a transition-metal-catalyst-free hydrosilylation process.

Many other alkene-insertion reactions into a silicon–heteroatom bond, such as silylstannylation,<sup>[3b]</sup> have also been described as synthetically useful transformations, although such reactions generally require transition-metal catalysts. Thus, we were interested in extrapolating our system to other silylene–phosphine complexes featuring a silicon(II)–heteroatom bond, such as a Si<sup>II</sup>–Sn bond. Herein, we report that alkene insertion into the Si<sup>II</sup>–Sn bond of trimethylstannyl-substituted silylene–phosphine complexes **1-Sn** takes place without any catalyst and under very mild conditions. Of particular interest is the reversibility of the insertion reaction even at room temperature.

The trimethylstannyl-substituted silylene complexes **1-Sn** can be prepared readily from the corresponding chlorosilylene<sup>[18]</sup> derivatives by treatment with one equivalent of trimethylstannyl-lithium. Products **1a-Sn** (81 % yield) and **1b-Sn** (85 % yield) could both be isolated in the solid state and were characterized in solution as well as by X-ray diffraction analysis (Figure 1, top).<sup>[19]</sup> Complex **1a-Sn** slowly reacted with ethylene gas (10 bar) at room temperature to



**Scheme 1.** Reversible alkene-insertion reactions into the Si–Sn bond of trimethylstannyl-substituted silylene–phosphine complexes **1-Sn**.

give the corresponding alkyl-substituted silylene **2a-Sn** (Scheme 1). When the reaction was monitored by <sup>31</sup>P NMR spectroscopy, total conversion was observed after 24 h, and none of the [2+1] cycloadduct intermediate was detected. The new silylene **2a-Sn** was stable at room temperature under inert conditions and could be isolated as pale-yellow crystals in high yield (87 %).

<sup>31</sup>P NMR spectroscopy of **2a-Sn** revealed two singlets ( $\delta$  = 82.2 and 80.1 ppm, 84:16) in agreement with the presence of

[\*] Dr. R. Rodriguez, Dr. Y. Contie, Dr. D. Gau, Dr. A. Baceiredo, Dr. T. Kato  
Université de Toulouse, UPS, and CNRS, LHFA UMR 5069  
31062 Toulouse Cedex 9 (France)  
E-mail: kato@chimie.ups-tlse.fr  
Homepage: <http://hfa.ups-tlse.fr>

Dr. N. Saffon-Merceron  
Université de Toulouse, UPS, and CNRS, ICT FR2599  
31062 Toulouse (France)

Dr. K. Miqueu, Dr. J.-M. Sotiropoulos  
Université de Pau et des Pays de l'Adour, IPREM (UMR CNRS 5254)  
Technopôle Hélioparc, 64053 Pau Cedex 09 (France)

[\*\*] We are grateful to the CNRS, the ANR (NOPROBLEM), and the European Research Council (ERC Starting Grant agreement no. 306658) for financial support of this research.

Supporting information for this article is available on the WWW under <http://dx.doi.org/10.1002/ange.201303705>.

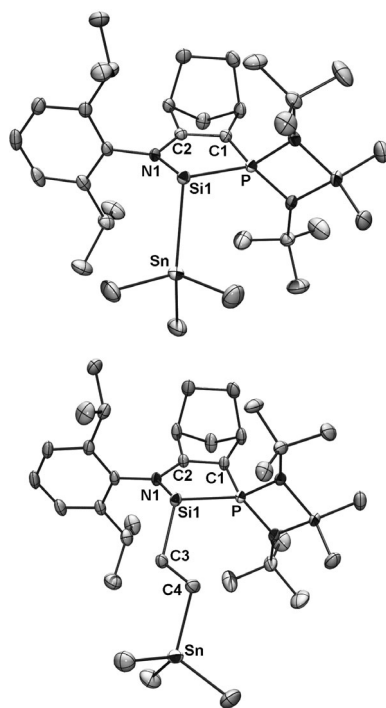


**Figure 1.** Molecular structure of **1a-Sn** (top) and **2a-Sn** (bottom). Thermal ellipsoids represent 30% probability. H atoms and disordered atoms are omitted for clarity. Selected bond lengths [Å] and angles [°]: **1a-Sn**: Si1–P 2.305(2), Si1–N1 1.848(2), Si1–Sn 2.612(1), N1–Si1–P 88.80(7), N1–Si1–Sn 112.76(7), P–Si1–Sn 105.00(3); **2a-Sn**: Si1–P 2.322(1), Si1–N1 1.850(2), Si1–C3 1.891(3), Sn–C4 2.145(2), C3–C4 1.542(3), N1–Si1–C3 105.25(10), N1–Si1–P 88.32(6), C3–Si1–P 105.56(9), Si1–C3–C4 109.45(18), C3–C4–Sn 114.29(17).

a pair of diastereomers, although the starting silylene **1a-Sn** was present as a single diastereomer ( $\delta = 87.1$  ppm). The major isomer was fully characterized by NMR spectroscopy, and the insertion of ethylene into the Si<sup>II</sup>–Sn bond was clearly indicated by the typical  $^{119}\text{Sn}$  NMR chemical shift at  $\delta = 3.8$  ppm ( $^4J_{\text{Sn,P}} = 3.8$  Hz) for a tetralkylstannane fragment. This signal differs significantly from that observed for **1a-Sn**, which features a Si–Sn bond ( $\delta = -104.7$  ppm,  $^2J_{\text{Sn,P}} = 81.2$  Hz).<sup>[20]</sup> The inserted ethylene fragment exhibited two CH<sub>2</sub> signals in the  $^{13}\text{C}$  NMR spectrum, at  $\delta = 5.9$  ppm ( $^3J_{\text{C,P}} = 7.3$  Hz) and at  $\delta = 12.7$  ppm. The  $^{29}\text{Si}$  NMR spectrum of silylene **2a-Sn** showed a doublet at  $\delta = -1.1$  ppm with a typical large coupling constant  $^1J_{\text{Si,P}} = 186.0$  Hz;<sup>[15]</sup> this signal is very similar to that observed for **1a-Sn** ( $\delta = -26.0$  ppm,  $^1J_{\text{Si,P}} = 190.4$  Hz). The structure of **2a-Sn** was unambiguously confirmed by X-ray diffraction analysis (Figure 1, bottom).<sup>[19]</sup>

The reaction of **1a-Sn** with ethylene was reversible. The evolution of a pure sample of **2a-Sn** in solution at different temperatures was monitored by  $^{31}\text{P}$  NMR spectroscopy, which indicated that the regeneration of **1a-Sn** starts at 85 °C (**2a-Sn/1a-Sn** 85:15), and that the proportion of the starting silylene **1a-Sn** increases with temperature (Figure 2). Above 85 °C, the ratio **2a-Sn/1a-Sn** is temperature-dependent (Table 1), which indicates that the reaction is at equilibrium under these conditions. The silylene complex **1b-Sn** with

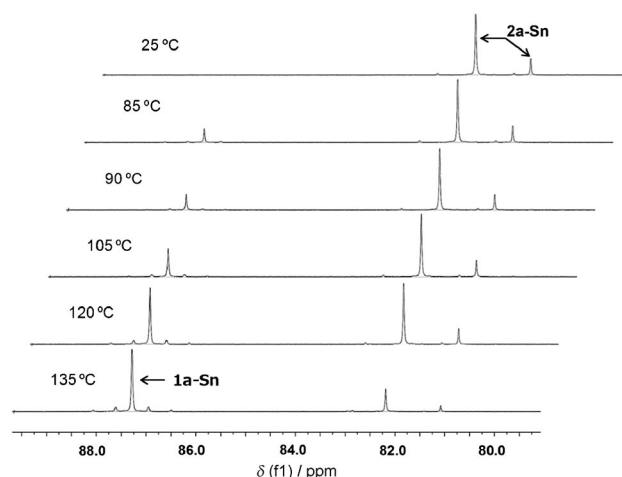


**Figure 2.**  $^{31}\text{P}\{^1\text{H}\}$  NMR spectroscopy of isolated **2a-Sn** at different temperatures (25–135 °C) in  $\text{C}_6\text{D}_6$  under Ar (4 bar).

**Table 1:** Proportions of **1-Sn** and **2-Sn** in the presence of ethylene (4 bar) in  $\text{C}_6\text{D}_6$  at different temperatures.

T [°C]	25	85	90	105	120	135
<b>2a-Sn/1a-Sn</b> <sup>[a]</sup>	100:0	85:15	81:19	71:29	53:47	28:72
T [°C]	25	40	50	60	70	80
<b>2b-Sn/1b-Sn</b> <sup>[a]</sup>	99:1	97:3	89:11	79:21	51:49	13:87

[a] The ratio was determined by  $^{31}\text{P}$  NMR and  $^1\text{H}$  NMR spectroscopy.

smaller substituents reacted with ethylene much faster, and the reaction was complete within 15 min at room temperature (Scheme 1). More interestingly, in this case, the equilibrium was observed at room temperature. As expected, the Gibbs free energies for these reactions are quite small ( $\Delta G_{85^\circ\text{C}} = -5.21$  kcal mol<sup>-1</sup> for **1a-Sn** and  $\Delta G_{25^\circ\text{C}} = -6.43$  kcal mol<sup>-1</sup> for **1b-Sn**).

The silylene complex **1a-Sn** also reacted with styrene at 45 °C to afford the corresponding alkene-inserted silylene **3a-Sn-X** (X = H; Figure 3). The reaction proceeded regioselectively in an anti-Markovnikov manner and was also an equilibrium process. Indeed, the ratio **3a-Sn-H/1a-Sn** at 45 °C depended strongly on the relative amount of styrene. At this temperature, the equilibrium is slightly shifted toward **1a-Sn**, and therefore an excess amount of styrene (36 equiv) was required to reach 90% conversion at 45 °C. The Gibbs free energy at 45 °C is only slightly negative ( $\Delta G_{45^\circ\text{C}} = -0.680$  kcal mol<sup>-1</sup>). This reaction of **1a-Sn** was also tested with various *p*-substituted styrenes. In all cases, the reaction proceeded in an anti-Markovnikov manner. In the case of the reaction with *p*-fluorostyrene, the structure of product **3a-Sn-F** was confirmed by X-ray diffraction analysis.<sup>[19,21]</sup> The reversibility of the process was observed at 45 °C with electron-poor styrenes (X = H, F, Cl), whereas slight thermal activation was required to reach the equilibrium (60 °C) in the case of more electron rich styrenes (X = Me, OMe; Figure 3). Thus, the equilibrium constant is strongly related to the nature of the styrene substituent (Figure 3A), and the reaction follows the Hammett correlation (Figure 3B).<sup>[22]</sup>

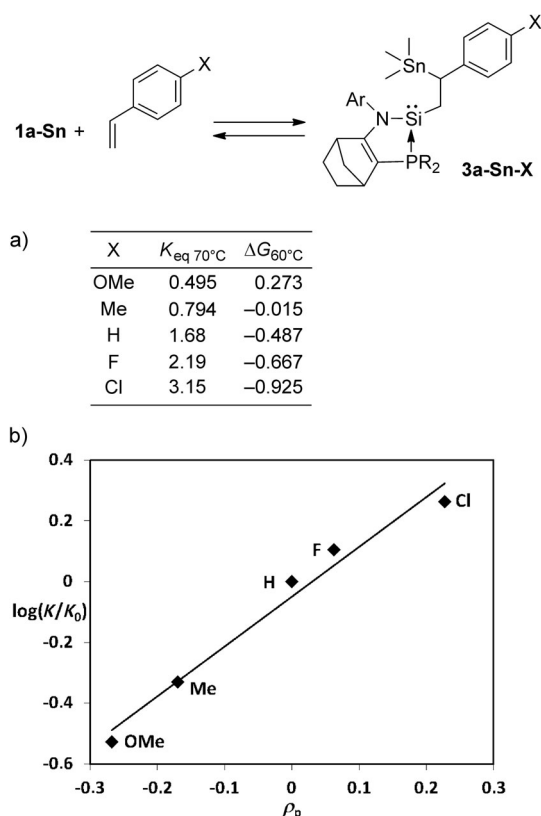


**Figure 3.** a) Equilibrium constant ( $K_{eq, 70^\circ C}$ ) and Gibbs free energy ( $\Delta G_{60^\circ C}$ ) and b) Hammett plot for the reaction of **1a-Sn** with several *p*-substituted styrene derivatives.

The positive value of the reaction constant ( $\rho$ ) in the Hammett equation [ $\log(K/K_0) = \rho\rho$ ] indicates that the insertion reaction is favored for electron-deficient styrenes, probably owing to the strongly nucleophilic silylene character of **1a-Sn**.<sup>[23]</sup>

To gain insight into these experimental results, we performed DFT calculations on the reaction of silylene complexes **1a-E** ( $E = H, SnMe_3$ ) with ethylene (Figure 4). We reported previously that the reaction of **1a-H** with ethylene proceeds in two steps: 1) [2+1] cycloaddition at room temperature, and 2) migratory insertion of ethylene at  $80^\circ C$ .<sup>[17]</sup> However, no intermediate was observed experimentally in the reaction between **1a-Sn** and ethylene. Nevertheless, calculations predict that the reaction of **1a-Sn** should also proceed in two steps (Figure 4). In this case, the intermediate was not observed because the rate-limiting step is the first step, the [2+1] cycloaddition, whereas in the case of **1a-H**, the rate-determining step is the insertion of ethylene. As expected, both steps (insertion/ $\beta$  elimination) for **1a-Sn** are almost thermoneutral ( $\Delta G = -5.8 \text{ kcal mol}^{-1}$ ) and present relatively small energy barriers, in good agreement with the experimental results (reversibility under mild conditions). In contrast, the migratory-insertion step for **4a-H** costs more energy ( $\Delta G^\ddagger = 26.2 \text{ kcal mol}^{-1}$ ). Besides, the reaction is strongly exergonic ( $\Delta G(2a-H-1a-H) = -15.6 \text{ kcal mol}^{-1}$ ), which explains the lack of reversibility of the reaction for **1a-H**. The difference observed between the two silylene

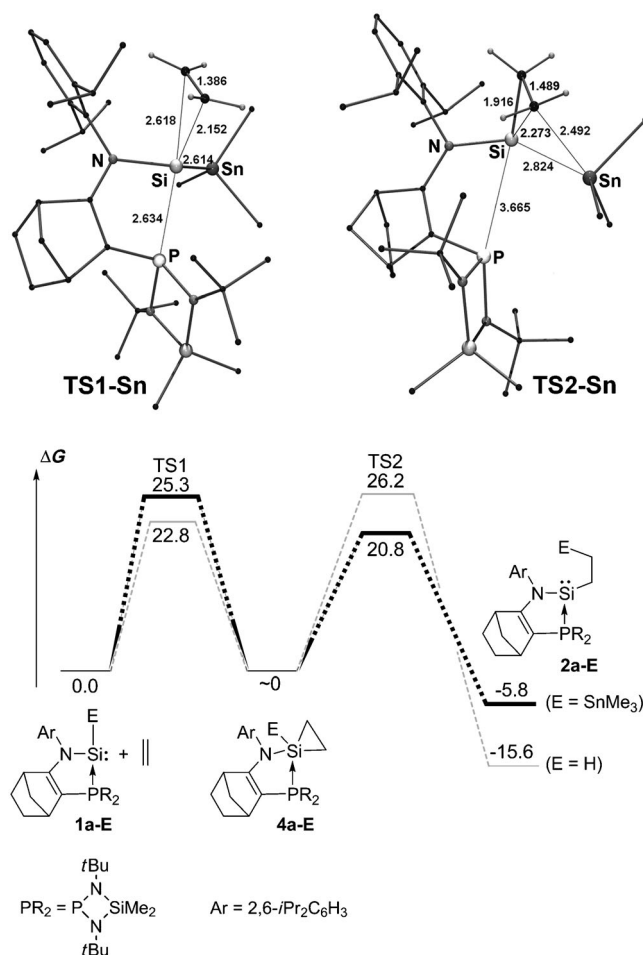


**Figure 4.** Calculated reaction profiles (Gibbs energies in  $\text{kcal mol}^{-1}$ ) for the ethylene-insertion reactions with silylene complexes **1a-Sn** and **1a-H** at the level of M06-SDD for Sn and 6-31G(d,p) for all other atoms.

complexes may be related to the bond energies involved in the process. Indeed, the two bonds involved in the reaction of **1a-Sn** are considerably weaker (Sn-Si:  $45 \text{ kcal mol}^{-1}$ , Sn-C:  $43 \text{ kcal mol}^{-1}$ ) than those in the case of **1a-H** (H-Si:  $76 \text{ kcal mol}^{-1}$ , H-C:  $98 \text{ kcal mol}^{-1}$ );<sup>[24]</sup> thus the energy barrier for the second migratory-insertion step and the gain in energy are lower for the formation of **2a-Sn** (formation of two  $\sigma$  bonds (Si-C and E-C) and loss of a  $\sigma$  bond (E-Si) and a C-C  $\pi$  bond ( $41 \text{ kcal mol}^{-1}$ )). In contrast, the higher energy barrier for the first step in the case of **1a-Sn** could be attributed to increased steric congestion due to the much bulkier  $SnMe_3$  group. The reaction of **1a-Sn** with styrene should proceed through a similar two-step mechanism, because a higher reaction rate was observed for electron-poor styrenes ( $X = F, Cl$ ), in agreement with a first rate-limiting step involving a nucleophilic silylene.<sup>[23]</sup>

In conclusion, we have successfully demonstrated the first reversible alkene-insertion reaction into  $Si^{II}$ -Sn bonds. This reaction takes place under mild conditions without any transition-metal catalyst. Theoretical studies indicated that the insertion reaction proceeds in two steps (oxidative addition-migratory insertion) and thus revealed that silycon(II)-phosphine complexes can behave like transition-

metal complexes. Calculations also indicated that each step of the reaction is thermoneutral and proceeds with a relatively small energy barrier, which explains the reversibility of the process under mild conditions. This particular energy profile in which divalent and tetravalent silicon species occur at the same energy level is probably the consequence of a particular phosphine-ligand effect that efficiently stabilizes  $\text{Si}^{\text{II}}$  species without loss of reactivity. Other systems are under active investigation.

Received: April 30, 2013

Published online: July 1, 2013

**Keywords:** cycloaddition · phosphorus · silicon · silylenes · ylides

- [1] a) R. H. Grubbs, G. W. Coates, *Acc. Chem. Res.* **1996**, *29*, 85; b) S. D. Ittel, L. K. Johnson, M. Brookhart, *Chem. Rev.* **2000**, *100*, 1169; c) V. C. Gibson, S. K. Spitzmesser, *Chem. Rev.* **2003**, *103*, 283.
- [2] *Metal-Catalysis in Industrial Organic Processes* (Eds.: G. P. Chiusoli, P. M. Maitlis), RSC Publishing, Cambridge, UK, **2006**.
- [3] a) I. P. Beletskaya, C. Moberg, *Chem. Rev.* **1999**, *99*, 3435; b) M. Suginome, Y. Ito, *Chem. Rev.* **2000**, *100*, 3221.
- [4] a) I. P. Beletskaya, A. V. Cheprakov, *Chem. Rev.* **2000**, *100*, 3009; b) C. Amatore, A. Jutand, *Acc. Chem. Res.* **2000**, *33*, 314; c) R. F. Heck, *Acc. Chem. Res.* **1969**, *2*, 10; d) R. F. Heck, *Acc. Chem. Res.* **1979**, *12*, 146.
- [5] H. C. Brown, B. C. Subba Rao, *J. Am. Chem. Soc.* **1959**, *81*, 6423.
- [6] a) D. S. Matteson, *Stereodirected Synthesis with Organoboranes*, Springer, New York, **1995**, chap. 2.
- [7] a) M. P. Coles, R. F. Jordan, *J. Am. Chem. Soc.* **1997**, *119*, 8125; b) S. Dagorne, I. A. Guzei, M. P. Coles, R. F. Jordan, *J. Am. Chem. Soc.* **2000**, *122*, 274; c) E. Ihara, V. G. Young, Jr., R. F. Jordan, *J. Am. Chem. Soc.* **1998**, *120*, 8277; d) J. S. Kim, L. M. Wojcinski II, S. Liu, J. C. Sworen, A. Sen, *J. Am. Chem. Soc.* **2000**, *122*, 5668; e) M. Bruce, V. C. Gibson, C. Redshaw, G. A. Solan, A. J. P. White, D. J. Williams, *J. Chem. Soc. Chem. Commun.* **1998**, 2523.
- [8] G. Talarico, V. Busico, P. H. M. Budzelaar, *Organometallics* **2001**, *20*, 4721.
- [9] K. Ziegler, *Angew. Chem.* **1956**, *68*, 721.
- [10] a) A. Jana, H. W. Roesky, C. Schulzke, A. Döring, *Angew. Chem.* **2009**, *121*, 1126; *Angew. Chem. Int. Ed.* **2009**, *48*, 1106; b) A. Jana, H. W. Roesky, C. Schulzke, *Inorg. Chem.* **2009**, *48*, 9543.
- [11] a) A. Jana, D. Ghoshal, H. W. Roesky, I. Objartel, G. Schwab, D. Stalke, *J. Am. Chem. Soc.* **2009**, *131*, 1288; b) A. Jana, S. S. Sen, H. W. Roesky, C. Schulzke, S. Dutta, S. K. Pati, *Angew. Chem.* **2009**, *121*, 4310; *Angew. Chem. Int. Ed.* **2009**, *48*, 4246.
- [12] L. W. Pineda, V. Jancik, K. Starke, R. B. Oswald, H. W. Roesky, *Angew. Chem.* **2006**, *118*, 2664; *Angew. Chem. Int. Ed.* **2006**, *45*, 2602.
- [13] S. L. Choong, W. D. Woodul, C. Schenk, A. Stasch, A. F. Richards, C. Jones, *Organometallics* **2011**, *30*, 5543.
- [14] a) D. Gau, R. Rodriguez, T. Kato, N. Saffon-Merceron, F. P. Cossio, A. Baceiredo, *Chem. Eur. J.* **2010**, *16*, 8255; b) D. Gau, R. Rodriguez, T. Kato, N. Saffon-Merceron, A. Baceiredo, *J. Am. Chem. Soc.* **2010**, *132*, 12841.
- [15] D. Gau, T. Kato, N. Saffon-Merceron, F. P. Cossio, A. Baceiredo, *J. Am. Chem. Soc.* **2009**, *131*, 8762.
- [16] R. Rodriguez, D. Gau, T. Kato, N. Saffon-Merceron, A. De Cózar, F. P. Cossio, A. Baceiredo, *Angew. Chem.* **2011**, *123*, 10598; *Angew. Chem. Int. Ed.* **2011**, *50*, 10414.
- [17] R. Rodriguez, D. Gau, Y. Contie, T. Kato, N. Saffon-Merceron, A. Baceiredo, *Angew. Chem.* **2011**, *123*, 11694; *Angew. Chem. Int. Ed.* **2011**, *50*, 11492.
- [18] D. Gau, T. Kato, N. Saffon-Merceron, A. De Cózar, F. P. Cossio, A. Baceiredo, *Angew. Chem.* **2010**, *122*, 6735; *Angew. Chem. Int. Ed.* **2010**, *49*, 6585.
- [19] See the Supporting Information for the crystal data for **1a-Sn**, **2a-Sn**, and **3a-Sn-F**. CCDC 935560 (**1a-Sn**), 935561 (**2a-Sn**), and 935562 (**3a-Sn-F**) contain the supplementary crystallographic data for this paper. These data can be obtained free of charge from The Cambridge Crystallographic Data Centre via [www.ccdc.cam.ac.uk/data\\_request/cif](http://www.ccdc.cam.ac.uk/data_request/cif).
- [20] J. D. Kennedy, W. McFarlane, G. S. Pyne, B. Wrackmeyer, *J. Chem. Soc. Dalton Trans.* **1975**, 386.
- [21] See the Supporting Information.
- [22] For a review on Hammett substituent constants, see: C. Hansch, A. Leo, R. W. Taft, *Chem. Rev.* **1991**, *91*, 165.
- [23] The nucleophilic silylenoid character of phosphine-stabilized silylenes has been reported previously: see Ref. [14a].
- [24] Y.-R. Luo, *Comprehensive Handbook of Chemical Bond Energies*, CRC, New York, **2007**.